FTO demethylates m6A modifications in HOXB13 mRNA and promotes endometrial cancer metastasis by activating the WNT signaling pathway

Lin Zhang
Chinese Academy of Medical Sciences & Peking Union Medical College Hospital & peking union medical college

Yicong Wan
Nanjing Medical University first Affiliated Hospital

Zihan Zhang
Chinese Academy of Medical Sciences & Peking Union Medical College Hospital & peking union medical college

Yi Jiang
Nanjing Medical University First Affiliated Hospital

Jinghe Lang (✉ langjinghe@aliyun.com)
Chinese Academy of Medical Sciences and Peking Union Medical College https://orcid.org/0000-0002-5087-3788

Wenjun Cheng (✉ chengwenjun@jsph.org.cn)
Nanjing Medical University First Affiliated Hospital

Lan Zhu (✉ zhulan0330@aliyun.com)
Chinese Academy of Medical Sciences & Peking Union Medical College Hospital & peking union medical college

---

Research

Keywords: Endometrial cancer, FTO, HOXB13, m6A, Cancer metastasis

Posted Date: May 26th, 2020

DOI: https://doi.org/10.21203/rs.3.rs-30454/v1

Abstract

Background Abnormal FTO expression causes faulty m6A modifications in mRNA and affects tumor progression. However, the expression and function of FTO in endometrial cancer (EC) and the genes regulated by FTO remain unclear.

Methods qPCR detected the FTO expression level in EC tissues, and IHC staining determined the FTO protein expression in tissue arrays. FTO was stably overexpressed or knocked down in EC cell lines by lentiviruses. The biological roles of FTO in cancer cell metastasis and invasion were evaluated by wound-healing, Transwell assays and mouse intra-abdominal implantation models. mRNA-seq, RIP-seq, and MeRIP-seq were combined to comprehensively map the genes regulated by FTO. RNA pull-down, dual-luciferase reporter and RNA stability experiments confirmed that YTHDF2 regulates the metabolism of HOXB13 mRNA via m6A. Western blot analysis confirmed that HOXB13 regulates EC cell metastasis and invasion through the WNT signaling pathway.

Results FTO is more highly expressed in metastatic EC and can promote tumor metastasis and invasion in vivo and in vitro. By removing the m6A modification in the 3'UTR region of HOXB13, FTO abolishes m6A recognition by YTHDF2 and promotes the stability of HOXB13 mRNA and protein expression. High HOXB13 expression activates the WNT signaling pathway, promotes c-myc, snail, MMP2, MMP7, and MMP9 expression, and inhibits E-cadherin expression, leading to tumor metastasis and invasion.

Conclusions FTO promotes HOXB13 expression through m6A, activates the WNT signaling pathway, and promotes EC invasion and metastasis. FTO is a new potential target for the treatment of tumor metastasis.

Background

The incidence of obesity in the population is increasing, and epidemiological studies have shown that obesity is a high-risk factor for endometrial cancer (EC) [1]. Therefore, the incidence of EC is increasing annually. According to the clinicopathological characteristics, EC can be divided into type I and type II [2]. Type I is mainly endometrial adenocarcinoma, is considered to be related to estrogen stimulation and has the characteristics of slow progression and late metastasis [3]. Type II EC is mainly clear cell carcinoma and serous carcinoma. The tumor progresses rapidly, is often accompanied by resistance to hormone therapy, and tumor invasion and metastasis easily occur at an early stage. Therefore, the 5-year survival rate of patients is significantly reduced [4–5]. Research on the molecular mechanism of tumor invasion and metastasis is very important to improve the survival rate of patients.

m6A is the most common chemical modification in mammalian mRNA [6]. In the nucleus, m6A modifications on mRNA are dynamically regulated, and proteins such as METTL3/14 catalyze the formation of m6A modifications on specific RNAs by forming methyltransferase complexes. Therefore, they are also called “writers” [7–8]. The FTO and ALKBH5 proteins can remove m6A modifications from mRNA. These proteins are called “erasers” [9]. When mRNA matures, these m6A-modified mRNAs are

transported into the cytoplasm. Some proteins can specifically recognize m6A modifications and regulate mRNA metabolic processes. These proteins are called “readers” [10]. The YTHDF family of proteins are the first "reader" proteins that have been shown to recognize the m6A modification [11]. After YTHDF1 recognizes an m6A modification of mRNA, it can accelerate the translation process [12]. When YTHDF2 recognizes an m6A modification, it will promote the transportation of mRNA into the p-body, accelerate mRNA degradation, and inhibit protein translation [13]. It has been found that abnormal expression of these proteins exists in various tumors and affects the occurrence and progression of tumors [14].

FTO belongs to the non-heme Fe II/αKG-dependent dioxygenase AlkB protein family, and its expression is closely related to weight gain and obesity [15]. Knocking down FTO expression in animal models can suppress obesity and lead to growth retardation, while FTO overexpression can lead to increased food intake and obesity [16]. Previous studies have shown that abnormal expression of FTO has been found in various tumors and participates in the regulation of multiple biological behaviors [17–18]. However, FTO has recently been found to act as a demethylase, leading to m6A demethylation in mRNA and regulating mRNA metabolism. The relationship of this new molecular mechanism of FTO and cancer progression is still unclear.

In this study, we studied the regulatory effects of FTO on endometrial cancer (EC) invasion and metastasis and explored the molecular mechanism of tumor metastasis based on the m6A regulatory mechanism.

Materials And Methods

Patient samples

RNA samples from 96 EC patients were retained from our previous research, among them, there were 30 patients with metastasis and 66 patients without metastasis. This study was approved by the Institutional Review Board (the First Affiliated Hospital of Nanjing Medical University).

Quantitative real-time PCR analysis

Briefly, RNA samples were reverse transcribed to cDNA by reverse transcriptase (TaKaRa, Tokyo, Japan). Gene expression was detected using a quantitative PCR kit (TaKaRa) and a 7900HT real-time instrument (ABI, CA, USA). Experimental procedures followed the manufacturers’ protocols. The primers are listed in Table S1. The transcript levels were analyzed using the $2^{-\Delta\Delta CT}$ method, and the expression of β-actin was used as an internal control.

Tissue array and immunohistochemistry (IHC)

A total of 142 tumor samples were enrolled in this study, including 66 endometrial tumor samples (without metastases), 30 intrauterine tumor samples (with metastases), 24 abdominal metastatic samples, and 22 lymph node metastasis samples. The IHC protocol was similar to that used in our

previous research [19]. Briefly, after paraffin embedding, sectioning, dewaxing, antigen retrieval and serum blocking, the samples were stained with antibodies. The antibody information is listed in Table S2. IHC staining was semiquantitatively evaluated based on the staining intensity and percentage of positive cells. The staining intensity was scored as 0 (negative), 1 (weakly positive), 2 (moderately positive), or 3 (strongly positive). The percentage of positive cells was scored as 1 (0%–10%), 2 (11%–50%), 3 (51%–80%), or 4 (81%–100%). The final score for each section was determined by multiplying the staining intensity score by the percentage staining score. IHC staining was independently scored by two pathologists, and the average was calculated.

Cells and cell culture

The human EC cell lines AN3CA and KLE were purchased from the China Center for Type Culture Collection (CATCC). Cells were cultured as described in our previous study [19].

Subcellular fractionation analysis

Protein fractionation of nuclear extracts was performed by using NE-PER Nuclear and Cytoplasmic Extraction Reagents (Thermo Fisher, CA, USA) according to the manufacturer's instructions.

Western blotting (WB)

Cells were washed twice in prechilled PBS and lysed in lysis buffer (100 mmol/L NaCl, 50 mmol/L Tris (pH 8.0), 1% NP-40, 0.1% SDS, 0.5 mM EDTA and 1× proteinase inhibitor cocktail). Lysates were centrifuged at 12500 g. Supernatants were collected, and proteins were denatured using LDS buffer (Thermo Fisher). Protein samples were separated by SDS-PAGE and transferred to a PVDF membrane. Membranes were blocked with 5% skim milk and sequentially incubated with primary and secondary antibodies. The antibody information is listed in Table S2. The immunoblot was developed using ChemiDoc (Bio-Rad) and ECL (Bio-Rad).

Lentivirus construction and infection, plasmid and siRNA transfection

The lentivirus-mediated gene overexpression or knockdown vector system was packed by Hanbio and included lentiviral vectors carrying FLAG and puromycin tags. Cells were cultured in six-well plates, and lentiviruses were added to each well. Empty lentiviral vectors served as a negative control, and noninfected cells served as a control group. After 48 h, the cells were cultured in 5 μg/ml puromycin to screen for cells with stable gene expression. Gene expression was verified by RT-PCR and WB. The HOXB13 CDS region was cloned into pcDNA 3.1 to construct an overexpression vector. HOXB13-specific siRNAs were synthesized by Tsingke. Cells were transfected with expression vector and siRNA using lipofectamine 3000 (Invitrogen, MI, USA) according to the manufacturer’s protocol. The oligo sequences are listed in Table S1.

Inhibition of the WNT signaling pathway

We used ICG-001 (Selleck, MI, USA) to inhibit the activity of the WNT signaling pathway in cells. The drug was diluted to a 10 mM stock solution with DMSO and stored at -20 °C. The medium was used to dilute the stock solution to the working concentration (10 μM).

Wound-healing assays

EC cells were seeded in a six-well plate after the indicated treatment. When the cells density reached 90%, a plastic pipette tip was used scratch the cell surface. PBS was used to wash the cell debris two times. Serum-free medium was added to each well for culture. After 48 h, the cells were photographed for analysis of the cell migration ability.

Transwell assay

A modified two-chamber migration assay was used to verify the cell invasion ability. Fifty microliters of 1:5 diluted Matrigel (BD, MA, USA) was added to the chamber (pore size: 8 μm; Corning, NY, USA) and placed in a 37 °C incubator for Matrigel solidification. After the indicated treatment, the designated cells were suspended in serum-free medium. 2×10^4 EC cells were seeded in the upper chamber, and 500 μl of medium containing 20% serum was added into the lower chamber. After the cells were cultured for 24 h, the cells were fixed with 4% paraformaldehyde, and a cotton swab was used to carefully wipe the cells in the upper chamber before photographs were taken.

RNA-binding protein immunoprecipitation sequencing and quantitative PCR (RIP-seq and RIP-qPCR)

To detect RNAs that bind to the FTO protein, an EZ-Magna RIP™ RNA-Binding Protein Immunoprecipitation Kit (Millipore, CA, USA) was used according to the manufacturer's protocol. Briefly, AN3CA cells (1×10^7) were washed in PBS twice and then lysed in 500 μl IP lysis buffer (containing 1x protease inhibitor cocktail and 5 μl RNase inhibitor). The supernatant was collected by centrifugation, and 10% was kept as the input sample. An anti-Flag antibody (5 μg) and a magnetic beads complex (40 μl) were added to the remaining 90% of the supernatant, and the samples were incubated at 4 °C overnight. Beads were washed with wash buffer and eluted using an RNA purification kit (Qiagen, Germany) according to the manufacturer's protocol. An Ultra II RNA Kit (NEB, MI, USA) was used to prepare the libraries according to the manufacturer's protocol. The samples were sequenced using the HiSeq PE150 platform. qPCR was performed by a 7900HT real-time instrument. The primers are listed in Table S1.

Methylated RNA immunoprecipitation sequencing (MeRIP-seq) and quantitative PCR (MeRIP-PCR)

Cells were washed in cold PBS twice, and an Oligotex Direct mRNA Midi/Maxi Kit (Thermo Fisher) was used to purify the mRNA according to the manufacturer's protocol. The mRNA concentration was quantified using a spectrophotometer, and 5 μg of mRNA was used for immunoprecipitation. A Magna MeRIP m^6A Kit (Millipore) was used for MeRIP according to the manufacturer's protocol. The samples

were sequenced with the HiSeq PE150 platform. qPCR was performed by a 7900HT real-time instrument. The primers are listed in Table S1.

RNA sequencing (RNA-seq) and quantitative PCR (qPCR)

Briefly, cells were washed twice with prechilled PBS. RNA was extracted using an RNeasy Mini Kit (Qiagen) according to the manufacturer's protocol. An Ultra II RNA Kit (NEB) was used to prepare the libraries according to the manufacturer's protocol. The libraries were sequenced with the HiSeq PE150 platform. qPCR was performed by a 7900HT real-time instrument. The primers are listed in Table S1.

RNA pull-down assays

The 5'-biotin RNA probe was synthesized by Tsingke. RNA probes contain either an m^6A base, an adenine base or a mutated guanine base. RNAiMAX reagents (Invitrogen) were used to transfect RNA probes into cells. After 48 h, cells were washed twice in cold PBS and lysed in 500 μl IP lysis buffer (containing 1x protease inhibitor cocktail and 5 μl RNase inhibitor). One-tenth of the supernatant was saved as the input sample. Then, 40 μl streptavidin beads (Invitrogen) were added to the remaining supernatant, and samples were incubated at room temperature for 2 h. The beads were eluted by 95% formamide at 95 °C for 2 min after five washes with IP wash buffer (Thermo Fisher). Protein samples were denatured by LDS buffer (Thermo Fisher) and analyzed by WB.

Luciferase reporter assays

We cloned a 3'UTR sequence containing the m6A site of HOXB13 into the pmirGLO reporter vector (Promega, CA, USA) and constructed a reporter gene vector with a single nucleotide mutation sequence (Fig. S3A). The detailed DNA sequences are listed in Table S1. Plasmids were verified by DNA sequencing. Cells seeded in 6-well plates were transfected with luciferase vectors using Lipofectamine 3000 (Invitrogen). Luciferase assays were performed using a Dual-Luciferase Reporter Assay System (Promega) according to the manufacturer's instructions. After 48 h, the firefly and Renilla luciferase activities in each well were evaluated.

RNA half-life assays

Cells were treated according to the experimental design, and actinomycin D (Sigma, CA, USA) was added at a concentration of 5 mg/ml. At the indicated time points (3hour, 6hour), the cells were lysed, and total RNA was extracted (Qiagen). RNA quantities were determined by qPCR. The RNA half-life was calculated according to a previous study [20].

In vivo tumorigenesis assay

Experimental animal procedures were approved by the Institutional Animal Care and committee (Peking Union Medical College). All animals received care in compliance with the 'Guide for the Care and Use of Laboratory Animals'. Female SCID-Berge mice (6 weeks old) were purchased from Vitalriver. AN3CA cells

with FTO overexpression or silencing or the appropriate controls (1×10^6) were injected into the lower abdominal cavity of mice (n=5 mice/group). After 4 weeks, the mice were sacrificed, and tumors were harvested, weighed and photographed. Tumors were fixed in 4% formaldehyde, paraffin-embedded and analyzed by IHC.

Sequencing data analysis

RNA-seq/RIP-seq datasheets were analyzed by HISAT2, featureCounts and DESeq2. MeRIP-seq data were analyzed by HISAT2 and exomePeak software. The correlation analysis of HOXB13 and YTHDF2 mRNA expression comes from TCGA database, and this work was performed by GEPIA (http://gepia.cancer-pku.cn).

Statistical analysis

SPSS 21.0 was used for all statistical analyses. Correlations between gene expression and clinicopathological data were analyzed by χ^2 and Fisher's exact test, respectively. Survival curves were generated using the Kaplan-Meier method. Data are expressed as the mean ± SD. Differences between two groups were analyzed by two-tailed Student's *t*-test. A p value < 0.05 indicated statistical significance.

Results

FTO expression is increased in metastatic EC samples

To explore the relationship between FTO expression and EC metastasis, we divided patients into metastatic and nonmetastatic groups. qPCR was used to detect the expression of FTO in EC samples, and FTO expression was higher in metastatic patients than in nonmetastatic patients (Fig. 1A). A tissue array was used to detect the protein expression of FTO in EC. The intrauterine samples were divided into metastatic and nonmetastatic groups according to whether there was metastasis. The expression of FTO in the metastatic group was significantly higher than that in the nonmetastatic group (Fig. 1B, Table S3A). In addition, the expression of FTO in peritoneal metastases and lymph node metastasis tumors was significantly higher than that in nonmetastatic tumors, but there was no difference in expression between various metastatic samples (Fig. 1C, Additional file 3: Table S3). This indicates that FTO expression is significantly increased in metastatic patients and may promote EC metastasis.

FTO promotes the invasion and metastasis of EC

To explore the role of FTO in regulating the invasion and metastasis of EC, we selected the AN3CA cell line derived from lymph node metastases and KLE cells with high metastatic potential for follow-up experiments. We used a lentiviral transfection vector to stably overexpress and knockdown FTO expression in cells (Additional file 8: Fig. S1). The wound-healing experiment showed that the metastatic ability was significantly increased after enhancing the expression of FTO in KLE cells. In contrast, after silencing FTO expression in KLE cells, cell metastasis was significantly reduced (Fig. 2A). A similar trend

was observed in the AN3CA cell line (Fig. 2B). In addition, Transwell assays were used to analyze the effect of FTO on invasion ability. Overexpression/knockdown of FTO expression led to increased/decreased cell invasion ability (Fig. 2C). Mouse peritoneal tumor models were used to explore the effect of FTO on metastasis in vivo. The intra-abdominal tumors were significantly larger than those in the control group after FTO overexpression and often formed multiple tumors. In contrast, after knockdown of FTO expression, the tumor weight was significantly reduced (Fig. 3A). The intensity of Ki-67 increased after FTO overexpression, in contrast, Ki-67 decreased upon FTO knockdown (Fig. 3B).

FTO removes the m6A modification in the 3'UTR region of HOXB13 mRNA

To explore the molecular mechanism of FTO promoting tumor invasion and metastasis, we stably knocked down the expression of FTO in AN3CA cells by shRNA. RNA-seq was employed to analyze the differentially expressed genes. There were 881 upregulated genes and 1696 downregulated genes (fold-change (FC) log2> 2, p <0.01) (Additional file 5: Table S5, Additional file 9: Fig. S2A). KEGG and GO analyses showed that the molecular functions of the differentially expressed genes were related to cell adhesion and metastasis (Fig. 4A, Additional file 9: Fig. S2B). Further, we used RIP-seq to detect the RNA bound to FTO and enriched to a total of 1316 genes (FC log2> 3). GO analysis showed that these RNAs were associated with apoptosis, cell adhesion and metastasis (Additional file 9: Fig. S2C). KEGG clustering showed that these genes were mainly enriched in the PI3K and MAPK signaling pathways (Additional file 9: Fig. S2D). We used MeRIP-seq to detect changes in m6A modifications in mRNA after silencing FTO expression. A total of 860 genes acquired a new m^6A peak, and 459 genes lost an m^6A peak (log2 FC> 1) (Fig. 4B). The most common motif of these enrichment peaks was DRACH (Fig. 4C), which is consistent with the results of a previous report. The positions of these peaks occur mainly near the stop codon (Fig. 4D). Because the main molecular function of FTO is to remove m^6A modifications, we therefore focused on the genes that acquired an m^6A peak. KEGG analysis showed that these genes were mainly enriched in the MAPK and WNT signaling pathways (Additional file 9: Fig. S2E).

To comprehensively display the gene mapping regulated by FTO through the m6A mechanism, we combined the analysis of the genes enriched in mRNA-seq, RIP-seq and MeRIP-seq. We screened 13 candidate genes (Fig. 4E). RIP-PCR, qPCR, MeRIP-PCR and WB were further used to verify the candidate genes. qPCR confirmed that the expression of HOXB13 was significantly reduced after silencing FTO expression. This trend was observed in both AN3CA and KLE cells (Fig. 4F). HOXB13 protein expression also decreased significantly after FTO knockdown (Fig. 4G). RIP-PCR experiments confirmed that HOXB13 mRNA can bind to the FTO protein with Flag labeling (Fig. 4H). Based on the MeRIP-seq results, we designed HOXB13 PCR primers targeted to the m6A modification peak (Additional file 1: Table 1). MeRIP-PCR showed that the m6A modification level increased after FTO knockdown (Fig. 4I). The m6A peak was located in the 3'UTR region of HOXB13 mRNA (Fig. 4J).

YTHDF2 promotes the decay of HOXB13 mRNA by recognizing the m6A peak

The m6A modification in mRNA requires recognition by the “Reader” protein. These reader proteins play a key role in regulating the mRNA metabolism. Previous report showed that YTHDF1 promotes translation by recognizing m6A, and YTHDF2 recognizes mRNA and often leads to mRNA degradation [13]. We found that FTO silencing could promote the appearance of the m6A peak in HOXB13 mRNA but was accompanied by a decrease in the mRNA expression of HOXB13. Therefore, we speculate that YTHDF2 can recognize this m6A modification and play a role in regulating HOXB13 mRNA. We used siRNA to silence the expression of YTHDF2 in cells. qPCR showed that the expression of HOXB13 mRNA increased (Fig. 5A). In addition, WB also confirmed that the protein expression of HOXB13 was significantly increased (Fig. 5B). Further, exogenous Flag-labeled YTHDF2 protein was used for RIP experiments, and the results confirmed that HOXB13 mRNA can bind to YTHDF2 (Fig. 5C). Since binding of the YTHDF2 protein to mRNA leads to RNA degradation, we used the actinomycin D experiment to verify the RNA stability. The half-life of HOXB13 mRNA increased significantly after knockdown of YTHDF2 (Fig. 5D). Moreover, we observed a decrease in the half-life of HOXB13 mRNA after silencing FTO (Fig. 5E). This suggests that FTO may regulate HOXB13 mRNA degradation through the m6A mechanism, and this mechanism may be mediated by YTHDF2.

To identify the biological function of the HOXB13 mRNA 3' UTR sequence, we performed luciferase reporter assays using a reporter vector containing either the wild-type or mutant 3' UTR sequence. In AN3CA cells with normal YTHDF2 protein expression, the luciferase reporter activity was significantly decreased in cells transfected with the wild-type construct, indicating that the sequence weakened the mRNA stability (Fig. 5F). The luciferase activity of cells transfected with the wild-type construct increased significantly after silencing YTHDF2. In addition, after silencing YTHDF2, no significant difference in the fluorescence intensity of cells was detected with wild-type or mutant vectors (Fig. 5F). This result indicates that the 3’UTR region is important for HOXB13 mRNA stability. We next aimed to explore whether YTHDF2 recognizes the 3’UTR region of HOXB13 mRNA via the m6A mechanism. According to the results of MeRIP-seq, we synthesized three RNA probes consisting of the 3'UTR sequence of HOXB13 mRNA, but each probe contained an m6A or m6A mutation (Fig. 5G). RNA pull-down experiments confirmed that YTHDF2 bound to the m6A site but had a weaker binding capacity to non-m6A sites (Fig. 5H). These results indicate that YTHDF2 recognizes the HOXB13 mRNA 3' UTR region in an m6A-dependent manner.

HOXB13 promotes the invasion and metastasis of EC

To explore whether HOXB13 could regulate endometrial cell invasion and metastasis, we constructed HOXB13 expression vectors and siRNA to enhance or knockdown HOXB13 expression. Overexpression of HOXB13 can promote the metastasis of KLE cells, while silencing the expression of HOXB13 leads to a decrease in metastasis (Fig. 6A). This trend was also observed in AN3CA cells (Fig. 6B). Transwell assays were used to analyze the effect of HOXB13 on invasion ability. Overexpression/knockdown of HOXB13 expression led to increased/decreased cell invasion ability (Fig. 6C). This indicates that HOXB13 has the ability to promote the invasion and metastasis of EC in vitro.

Further, we used IHC to detect the expression of HOXB13 in an EC tissue array to study the effect of HOXB13 on tumor metastasis, and the grouping is the same as before. HOXB13 expression was significantly higher in metastatic tumors than in nonmetastatic tumors (Fig. 6D, Additional file 4: Table S4). The expression of HOXB13 in peritoneal metastases and lymph node metastatic tumors was significantly higher than that in nonmetastatic tumors, but there was no difference in expression between various metastatic samples (Fig. 6D, Additional file 4: Table S4). This indicates that HOXB13 expression is significantly increased in metastatic patients. Since YTHDF2 can promote the degradation of HOXB13 mRNA, we speculate that there is a negative correlation between gene expression in tissues. Correlation analysis showed that YTHDF2 and HOXB13 had a negative correlation in mRNA expression by using TCGA data (Additional file 10: Fig. S3B).

HOXB13 promotes EC metastasis and invasion by activating the WNT signaling pathway

HOXB13 is a homeobox transcription factor that can directly regulate gene expression. The KEGG pathway was mainly enriched in the MAPK, PI3K, and WNT pathways after FTO knockdown. The activation of the WNT signaling pathway is highly related to metastasis in various cancers. To explore whether HOXB13 promotes tumor metastasis through the WNT signaling pathway, we added WNT pathway-specific inhibitors to AN3CA and KLE cells. Wound-healing and Transwell assays showed that the metastatic and invasive abilities of AN3CA cells were significantly reduced (Fig. 7A, B). Furthermore, we supplemented WNT signaling pathway inhibitors into HOXB13-overexpressing AN3CA cells. Wound-healing and Transwell experiments showed that the metastatic and invasive abilities of KLE cells were significantly reduced, and these trends were also detected in AN3CA cells (Fig. 7C, D). This indicates that the effect of HOXB13 in promoting EC invasion and metastasis can be inhibited by WNT signaling pathway inhibitors.

To detect the molecular mechanism of HOXB13 activation, the WNT signaling pathway was examined. We transfected the expression vector to overexpress the HOXB13 protein in the cells, and the time gradient showed that the concentration of β-catenin in the nucleus gradually increased (Fig. 7E). In contrast, when we silenced the expression of HOXB13 in cells, the concentration of β-catenin in the nucleus gradually decreased, while the concentration of phosphorylated β-catenin (Ser33/37) gradually increased (Fig. 7F). Furthermore, WB detected the expression of target genes downstream of the WNT signaling pathway. The expression of c-myc, snail, MMP2, MMP7 and MMP7 increased after HOXB13 overexpression. However, this trend may be blocked by adding WNT inhibitor (Fig. 7G).

Discussion

Invasion and metastasis are important biological behaviors that lead to the poor prognosis of cancer patients [21]. FTO expression is significantly increased in breast cancer, gastric cancer, melanoma, cervical cancer and other solid tumors [22]. High FTO expression in gastric cancer is positively correlated with tumor lymph node metastasis and promotes cancer invasion and metastasis [23]. FTO is highly expressed in lung cancer and is an independent factor affecting the prognosis of lung cancer. Decreasing

the expression of FTO in lung cancer cells can significantly inhibit tumor proliferation and invasion [24]. In this study, we found that FTO expression increased in EC, and FTO expression was positively correlated with tumor invasion and lymph node metastasis. Patients with high FTO expression had a worse prognosis, which was consistent with previous findings. Feng et al. reported that FTO expression is increased in EC [25]. However, high FTO expression is not related to tumor invasion and metastasis, which is not consistent with our report. The reasons for this discrepancy may include the following: (1) The populations enrolled in the two studies were different. (2) FTO expression is correlated with obesity, and BMI differences in patients may lead to discrepancies.

Previous studies have shown that HOXB13 can play a role in regulating tumor invasion and metastasis in a variety of tumors [26–27]. However, the function of HOXB13 in different tumor types is not consistent. HOXB13 promotes the occurrence of epithelial-mesenchymal transition (EMT) in ovarian cancer by inducing SLUG expression and enhances the ability of tumor metastasis [28]. In prostate cancer, HOXB13 promotes tumor cell invasion by reducing the expression of PDEF in the cell [29]. However, HOXB13 can inhibit the invasion of tumor cells by inhibiting the expression of ER-α in breast cancer [30]. In addition, the expression level of HOXB13 is reduced in colorectal cancer and malignant melanoma. Increasing the expression of HOXB13 can inhibit the proliferation of colon cancer and malignant melanoma [31–32]. This suggests that the role played by HOXB13 in the progression of different tumors is complex. In this study, we found that expression of HOXB13 in EC is increased in metastatic tumors and that expression of HOXB13 can promote tumor cell invasion and metastasis in vitro. These results indicate that HOXB13 plays a role in promoting tumor metastasis during tumor progression.

The expression of HOXB13 in tumor cells is regulated by various mechanisms. miR-7 can inhibit the expression of HOXB13 and regulate the migration of esophageal squamous cell carcinoma [33], while HOXB13-AS inhibits the expression of HOXB13 by methylating the HOXB13 promoter, affecting the proliferation of glioma [34]. MEIS1 promotes the proliferation of prostate cancer cells by extending the half-life of HOXB13 in prostate cancer [35]. In this study, we found for the first time that the m6A modification in HOXB13 mRNA can regulate the protein expression of HOXB13, and the expression of HOXB13 can activate the WNT signaling pathway and promote the expression of downstream genes, thereby enhancing tumor invasion and metastasis. These results provide new evidence for clarifying the molecular mechanism of HOXB13 in promoting tumor metastasis.

Obesity is a high-risk factor for EC, but the molecular mechanism between obesity and the biological behavior of EC cells has been unclear. Previous studies have shown that FTO expression is clearly related to obesity [36–37]. FTO was identified as a demethylase in 2011 and can “erase” the m6A modification on RNA [38]. However, the methylation mapping of FTO regulation in EC is not clear. In this study, we comprehensively displayed the m6A modification profile regulated by FTO in EC cells. This provides a new perspective for the further exploration of obesity and EC progression. Earlier studies showed that m6A-modified mRNAs are often unstable, mainly because YTHDF2 promotes RNA relocation to RNA decay sites and accelerates mRNA decay [39]. However, subsequent studies have found more proteins that can recognize m6A modifications and regulate mRNA metabolism, such as RNA translation, splicing

and stability [40]. FTO overexpression can erase the m6A site from the mRNA, resulting in faculty mRNA modifications and abolishing the RNA metabolism pathways mediated by various readers, ultimately affecting the mRNA function [41]. In this study, we found that FTO regulates m6A modification in HOXB13 mRNA, deprives HOXB13 degradation mediated by YTHDF2, promotes the expression of HOXB13, and accelerates EC cell metastasis. Nearly 1/3 of mRNAs have m6A modifications. The number of genes regulated by FTO through the m6A mechanism may be very large. In this study, 860 genes acquired a new m^6A peak, and 459 genes lost an m^6A peak after FTO knockdown, and these changes were accompanied by differences in mRNA expression. This indicates that FTO has a large number of target genes regulated by the m6A mechanism. More research is required to fully understand the molecular mechanism of FTO regulation of EC progression.

Conclusions

In this study, we found that the expression of FTO can promote the metastasis of EC. Mechanistically, FTO removed the m6A modification from HOXB13 mRNA and abolished the YTHDF2-mediated degradation of HOXB13, promoting HOXB13 protein expression and activates the WNT signaling pathway, and promotes EC invasion and metastasis (Fig. 8). FTO is a new potential target for the treatment of tumor metastasis.

Abbreviations

EC: Endometrial cancer; FTO: FTO Alpha-Ketoglutarate Dependent Dioxygenase; HOXB13: Homeobox B13; m6A: N6-Methyladenosine; MMP2: Matrix Metallopeptidase 2; MMP7: Matrix Metallopeptidase 7; MMP9: Matrix Metallopeptidase 9; UTR: Untranslated Region; YTHDF2:YTH N6-Methyladenosine RNA Binding Protein 2.

Declarations

Ethics approval

The study has been approved by the Ethics Committee of Jiangsu province Hospital. All experimental methods abided by the Helsinki Declaration. Experimental animal procedures were approved by the Institutional Animal Care and committee (Peking Union Medical College). All animals received care in compliance with the ‘Guide for the Care and Use of Laboratory Animals’.

Consent for publication

All authors are agree to publish our work to Journal of Experimental & Clinical Cancer Research.

Competing interests

The authors declare that they have no competing interests

Funding

This study was supported by the Young Scientists Fund of the National Natural Science Foundation of China (No. 81502243, 81702566), National Natural Science Foundation(No. 81872119), Chinese Academy of Medical Sciences innovation project (No. 2017-I2M-1-002), Innovative Team of Jiangsu Province(CXTDA2017008), 333 High-level Talents Training Project in Jiangsu Province (2019). Scientific Research Project of Jiangsu Province Maternal and Child Health Association (No.FYX201909), Key Young Medical Talents of Jiangsu Province (No.QNRC2016610).

Author contributions

L. Z., Y.C. W. Performed molecular biology, protein chemistry and statistical analysis. Z.H. Z. performed cell culture experiments and animal experiments. Y. J. Tested the human samples and were responsible for sample collection and patients fellow up. J.H. L., W.J. C., L. Z. supervised the study. All authors read and approved the final manuscript.

Availability of data and materials

All data generated or analyzed during this study are included in this published article [and its supplementary information files].

References

1. Katz A. CE: Obesity-Related Cancer in Women: A Clinical Review. Am J Nurs. 2019;119:34–41.
2. Carugno J. Clinical management of vaginal bleeding in postmenopausal women. Climacteric. 2020.
3. Dai Y, Wang Z, Wang J. Survival of microsatellite-stable endometrioid endometrial cancer patients after minimally invasive surgery: An analysis of the Cancer Genome Atlas data. Gynecol Oncol. 2020.
4. Han C, Altwerger G, Menderes G, Haines K, Feinberg J, Lopez S, et al. Novel Targeted Therapies in Ovarian and Uterine Carcinosarcomas. Discov Med. 2018;25:309–19.
5. Travaglino A, Raffone A, Stradella C, Esposito R, Moretta P, Gallo C, et al. Impact of endometrial carcinoma histotype on the prognostic value of the TCGA molecular subgroups. Arch Gynecol Obstet. 2020.
6. He L, Li H, Wu A, Peng Y, Shu G, Yin G. Functions of N6-methyladenosine and its role in cancer. Mol Cancer. 2019; 18.
7. Zaccara S, Ries RJ, Jaffrey SR. Reading, writing and erasing mRNA methylation. Nat Rev Mol Cell Bio. 2019;20:608–24.
8. Shi H, Wei J, He C. Where, When, and How: Context-Dependent Functions of RNA Methylation Writers, Readers, and Erasers. Mol Cell. 2019;74:640–50.
9. Zhao W, Qi X, Liu L, Ma S, Liu J, Wu J. Epigenetic Regulation of m(6)A Modifications in Human Cancer. Mol Ther-Nucl Acids. 2020;19:405–12.

10. Chen X, Zhang J, Zhu J. The role of m(6)A RNA methylation in human cancer. Mol Cancer. 2019; 18.
11. Zhu T, Roundtree IA, Wang P, Wang X, Wang L, Sun C, et al. Crystal structure of the YTH domain of YTHDF2 reveals mechanism for recognition of N6-methyladenosine. Cell Res. 2014;24:1493–6.
12. Wang X, Zhao BS, Roundtree IA, Lu Z, Han D, Ma H, et al. N-6-methyladenosine Modulates Messenger RNA Translation Efficiency. Cell. 2015;161:1388–99.
13. Huang T, Liu Z, Zheng Y, Feng T, Gao Q, Zeng W. YTHDF2 promotes spermagonial adhesion through modulating MMPs decay via m(6)A/mRNA pathway. Cell Death Dis. 2020; 11.
14. Huang H, Weng H, Chen J. m(6)A Modification in Coding and Non-coding RNAs: Roles and Therapeutic Implications in Cancer. Cancer Cell. 2020;37:270–88.
15. Smemo S, Tena JJ, Kim K, Gamazon ER, Sakabe NJ, Gomez-Marin C, et al. Obesity-associated variants within FTO form long-range functional connections with IRX3. Nature. 2014;507:371.
16. Jia G, Yang C, Yang S, Jian X, Yi C, Zhou Z, et al. Oxidative demethylation of 3-methylthymine and 3-methyluracil in single-stranded DNA and RNA by mouse and human FTO. Febs Lett. 2008;582:3313–9.
17. Gholamalizadeh M, Jarrahi AM, Akbari ME, Bourbour F, Mokhtari Z, Salahshoornezhad S, et al. Association between FTO gene polymorphisms and breast cancer: the role of estrogen. EXPERT REVIEW OF ENDOCRINOLOGY & METABOLISM. 2020.
18. Hu Y, Wang S, Liu J, Huang Y, Gong C, Liu J, et al. New sights in cancer: Component and function of N6-methyladenosine modification. Biomed Pharmacother. 2020; 122.
19. Zhang L, Wan Y, Jiang Y, Zhang Z, Shu S, Cheng W, et al. Overexpression of BP1, an isoform of Homeobox Gene DLX4, promotes cell proliferation, migration and predicts poor prognosis in endometrial cancer. Gene. 2019;707:216–23.
20. Huang H, Weng H, Sun W, Qin X, Shi H, Wu H, et al. Recognition of RNA N-6- methyladenosine by IGF2BP proteins enhances mRNA stability and translation. Nat Cell Biol. 2018;20:285.
21. Lewczuk L, Pryczynicz A, Guzinska-Ustymowicz K. Cell adhesion molecules in endometrial cancer - A systematic review. Adv Med Sci-Poland. 2019;64:423–9.
22. Deng X, Su R, Stanford S, Chen J. Critical Enzymatic Functions of FTO in Obesity and Cancer. Front Endocrinol. 2018; 9.
23. Li Y, Zheng D, Wang F, Xu Y, Yu H, Zhang H. Expression of Demethylase Genes, FTO and ALKBH1, Is Associated with Prognosis of Gastric Cancer. Digest Dis Sci. 2019;64:1503–13.
24. Liu J, Ren D, Du Z, Wang H, Zhang H, Jin Y. m(6)A demethylase FTO facilitates tumor progression in lung squamous cell carcinoma by regulating MZF1 expression. Biochem Bioph Res Co. 2018;502:456–64.
25. Zhu Y, Shen J, Gao L, Feng Y. Estrogen promotes fat mass and obesity-associated protein nuclear localization and enhances endometrial cancer cell proliferation via the mTOR signaling pathway. Oncol Rep. 2016;35:2391–7.

26. Brechka H, Bhanvadia RR, VanOpstall C, Vander Griend DJ. HOXB13 mutations and binding partners in prostate development and cancer: Function, clinical significance, and future directions. GENES DISEASES. 2017;4:75–87.
27. Ouhtit A, Al-Kindi MN, Kumar PR, Gupta I, Shanmuganathan S, Tamimi Y. Hoxb13, a potential prognostic biomarker for prostate cancer. Front Biosci. 2016;8:40–5.
28. Yuan H, Kajiyama H, Ito S, Chen D, Shibata K, Hamaguchi M, et al. HOXB13 and ALX4 induce SLUG expression for the promotion of EMT and cell invasion in ovarian cancer cells. ONCOTARGET. 2015;6:13359–70.
29. Kim I, Kang TW, Jeong T, Kim Y, Jung C. HOXB13 regulates the prostate-derived Ets factor: Implications for prostate cancer cell invasion. Int J Oncol. 2014;45:869–76.
30. Liu B, Wang T, Wang H, Zhang L, Xu F, Fang R, et al. Oncoprotein HBXIP enhances HOXB13 acetylation and co-activates HOXB13 to confer tamoxifen resistance in breast cancer. J Hematol Oncol. 2018; 11.
31. Ghoshal K, Motiwala T, Claus R, Yan P, Kutay H, Datta J, et al. HOXB13, a Target of DNMT3B, Is Methylated at an Upstream CpG Island, and Functions as a Tumor Suppressor in Primary Colorectal Tumors. Plos One. 2010; 5.
32. Maeda K, Hamada J, Takahashi Y, Tada M, Yamamoto Y, Sugihara T, et al. Altered expressions of HOX genes in human cutaneous malignant melanoma. Int J Cancer. 2005;114:436–41.
33. Li R, Ke S, Meng F, Lu J, Zou X, He Z, et al. CiRS-7 promotes growth and metastasis of esophageal squamous cell carcinoma via regulation of miR-7/HOXB13. Cell Death Dis. 2018; 9.
34. Xiong Y, Kuang W, Lu S, Guo H, Wu M, Ye M, et al. Long noncoding RNA HOXB13-AS1 regulates HOXB13 gene methylation by interacting with EZH2 in glioma. Cancer Med-Us. 2018;7:4718–28.
35. Johng D, Torga G, Ewing CM, Jin K, Norris JD, McDonnell DP, et al. HOXB13 interaction with MEIS1 modifies proliferation and gene expression in prostate cancer. Prostate. 2019;79:414–24.
36. Chang JY, Park JH, Park SE, Shon J, Park YJ. The Fat Mass- and Obesity-Associated (FTO) Gene to Obesity: Lessons from Mouse Models. Obesity. 2018;26:1674–86.
37. Mizuno TM. Fat Mass and Obesity Associated (FTO) Gene and Hepatic Glucose and Lipid Metabolism. Nutrients. 2018; 10.
38. Niu Y, Zhao X, Wu Y, Li M, Wang X, Yang Y. N6-methyl-adenosine (m6A) in RNA: an old modification with a novel epigenetic function. Genom Proteom Bioinform. 2013;11:8–17.
39. Wang X, He C. Reading RNA methylation codes through methyl-specific binding proteins. Rna Biol. 2014;11:669–72.
40. Boo SH, Kim YK. The emerging role of RNA modifications in the regulation of mRNA stability. Exp Mol Med. 2020;52:400–8.
41. Hirayama M, Wei F, Chujo T, Oki S, Yakita M, Kobayashi D, et al. FTO Demethylates Cyclin D1 mRNA and Controls Cell-Cycle Progression. Cell Rep. 2020; 31.

Supplemental Legends

Additional file 1: Table S1: Primers and oligos used in this study.

Additional file 2: Table S2：List of antibodies.

Additional file 3: Table S3: Association between FTO expression and clinicopathologic parameters

Additional file 4: Table S4: Association between HOXB13 expression and clinicopathologic parameters

Additional file 5: Table S5. mRNA-seq data after FTO knockdown.

Additional file 6: Table S6. Flag-FTO RIP-seq data.

Additional file 7: Table S7. MeRIP-seq data after FTO knockdown.

Additional file 8: Figure S1: FTO is stably overexpressed and silenced in AN3CA cells. PCR (Top) and WB (bottom) analysis of FTO overexpression or knockdown in AN3CA cells. FTO (+): Overexpression of FTO by lentiviruses. FTO (+) NC: Negative control lentiviral vector. FTO shRNA: knockdown of *FTO* by shRNA lentiviruses. FTO shRNA NC: Negative control shRNA lentiviruses. Error bars indicate means ± SDs, $^{**}P<0.01$.

Additional file 9: Figure S2. GO and KEGG analyses of mRNA-seq, RIP-seq and MeRIP-seq data. (A) Volcano graph showing differentially expressed genes in mRNA-seq. (B) GO analysis of differentially expressed genes in mRNA-seq. (C) GO analysis of the genes enriched by FTO RIP-seq. (D) KEGG cluster analysis of genes enriched by RIP-seq. (E) KEGG cluster analysis of the genes that acquired m6A peaks.

Additional file 10: Figure S3. Correlation analysis between HOXB13 and YTHDF2 expression. (A) Schematic diagram of the luciferase reporter gene vector. (B) Correlation analysis between HOXB13 and YTHDF2 expression based on TCGA data.

Figures

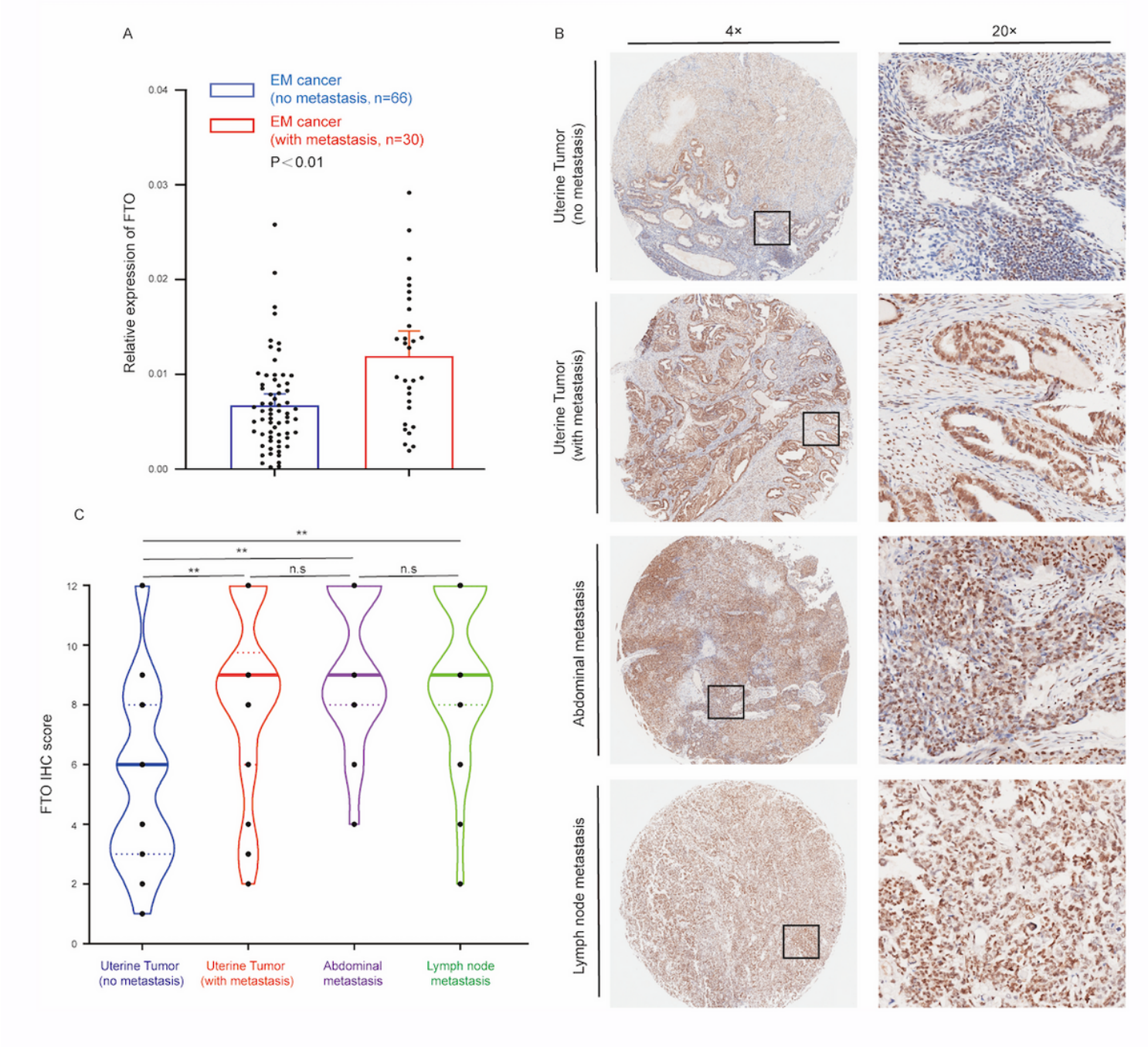

Figure 1

FTO is overexpressed in metastatic EC cancer. (A) FTO mRNA expression in metastatic EC (N=30) and nonmetastatic EC tissues (N=66). (B) Expression of the FTO protein in nonmetastatic EC tissue and different types of metastatic EC tissues. (C) The IHC score of the FTO protein in different EC samples. **P < 0.01, n.s indicates not significant.

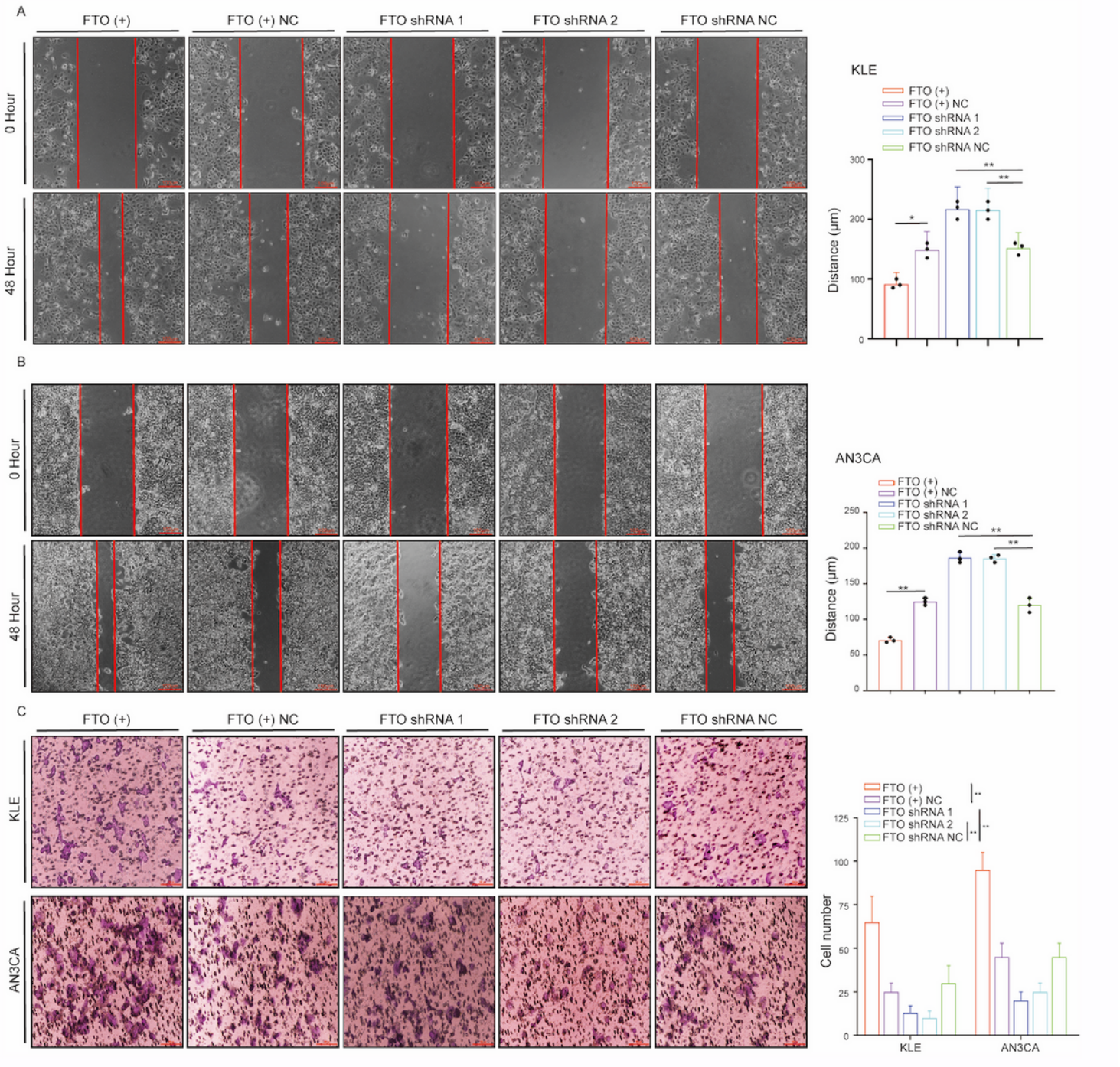

Figure 2

FTO promotes EC cell metastasis and invasion. (A) FTO overexpression and knockdown regulate cell migratory abilities in KLE cells according to wound-healing assays. (B) Wound-healing assays demonstrate that FTO regulates cell metastasis of AN3CA cells. (C) Effects of FTO overexpression and knockdown on cell invasive capacities by Transwell assays. FTO (+) NC: Negative control lentiviral vector. FTO shRNA: knockdown of FTO by shRNA lentiviruses. FTO shRNA NC: Negative control shRNA lentiviruses. Error bars indicate means ± SDs, **P<0.01.

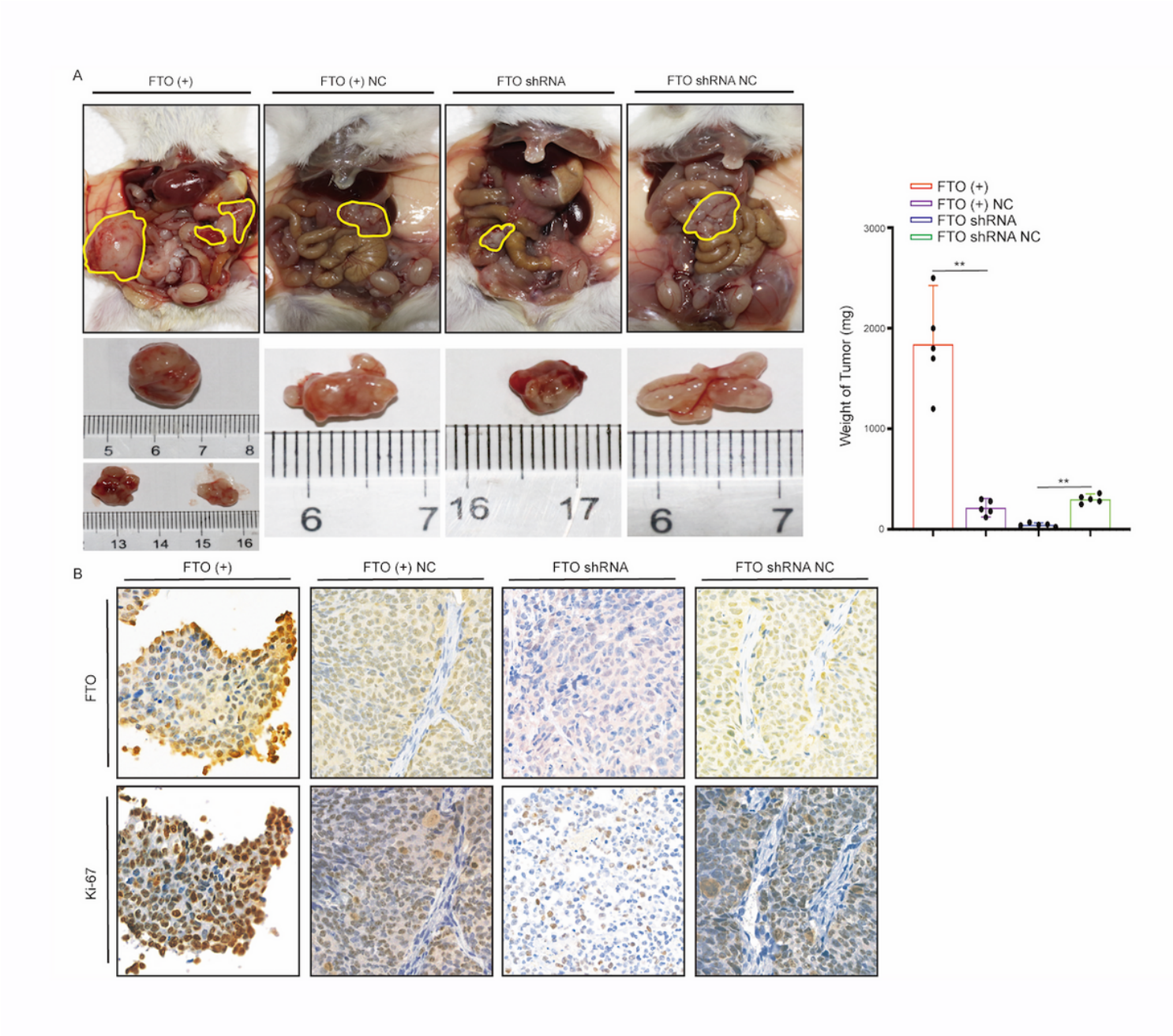

Figure 3

FTO promotes EC cell growth in vivo. (A) Weight of xenografts derived from AN3CA cells (n=5 mice/group). (B) IHC staining of FTO and Ki-67 in tumor samples from. Error bars indicate means ± SDs, **P<0.01.

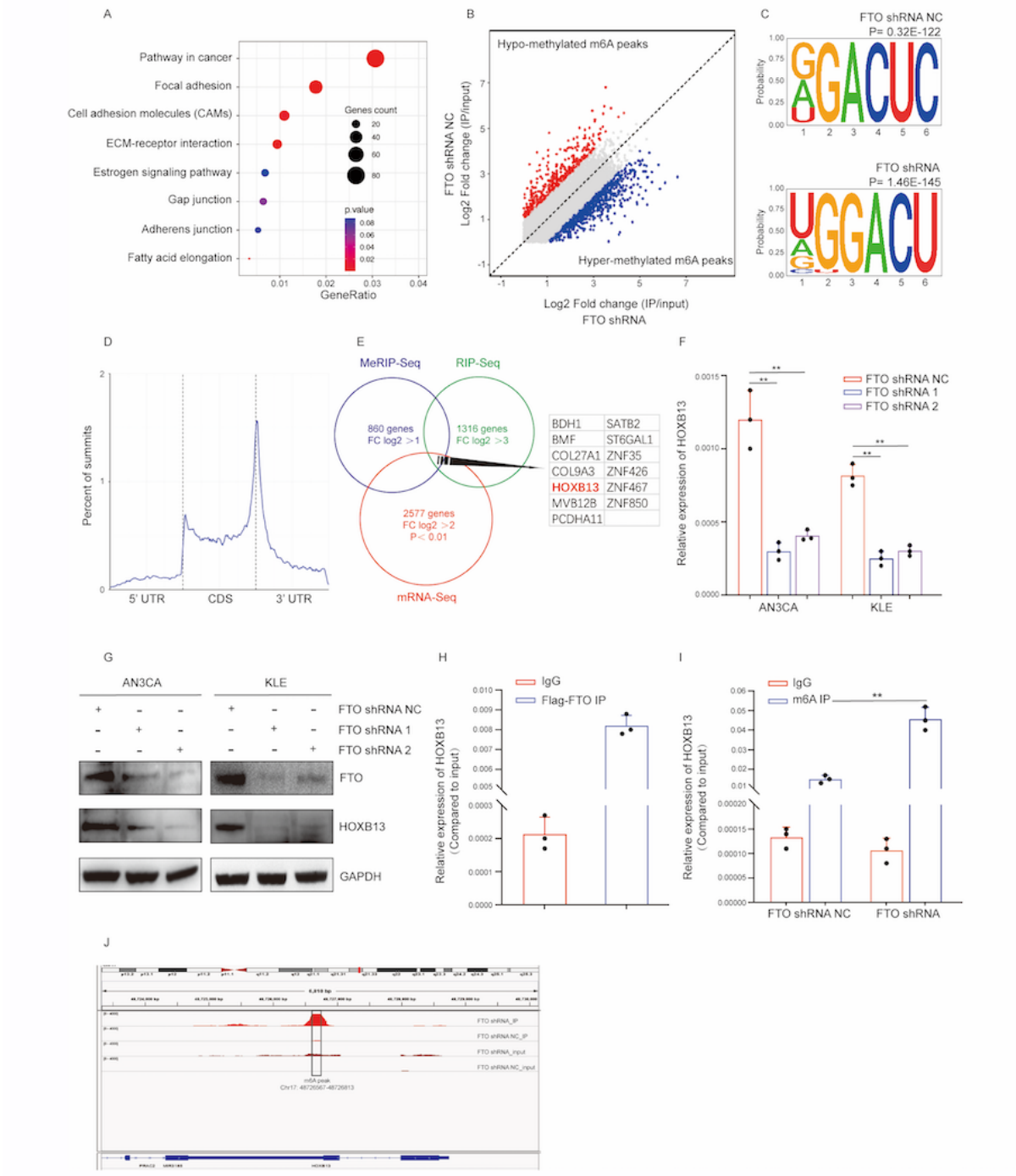

Figure 4

FTO recognizes and regulates m6A in HOXB13 mRNA. (A) KEGG enrichment map of genes specifically enriched by RNA-seq after FTO knockdown. (B) MeRIP-seq detects changes in m6A modifications in mRNA after silencing FTO expression. (C) Top motif identified by HOMER with m6A-seq peaks. (D) Distribution of new m6A peaks in mRNA detected by MeRIP-seq after knocking down FTO expression. (E) Venn diagram shows the genes enriched by MeRIP-seq, RNA-seq, and RIP-seq. (F, G) qPCR and WB

confirmed decreased HOXB13 mRNA after FTO knockdown in AN3CA and KLE cells. (H) RIP-PCR validates exogenous FTO binding to HOXB13 mRNA. (I) MeRIP-PCR confirmed that the m6A peak in the 3' untranslated region of HOXB13 mRNA was regulated by FTO. (J) The m6A peak in HOXB13 mRNA transcripts in FTO knockdown samples (IP and input) and the negative control (IP and input). Error bars indicate means ± SDs, **P<0.01.

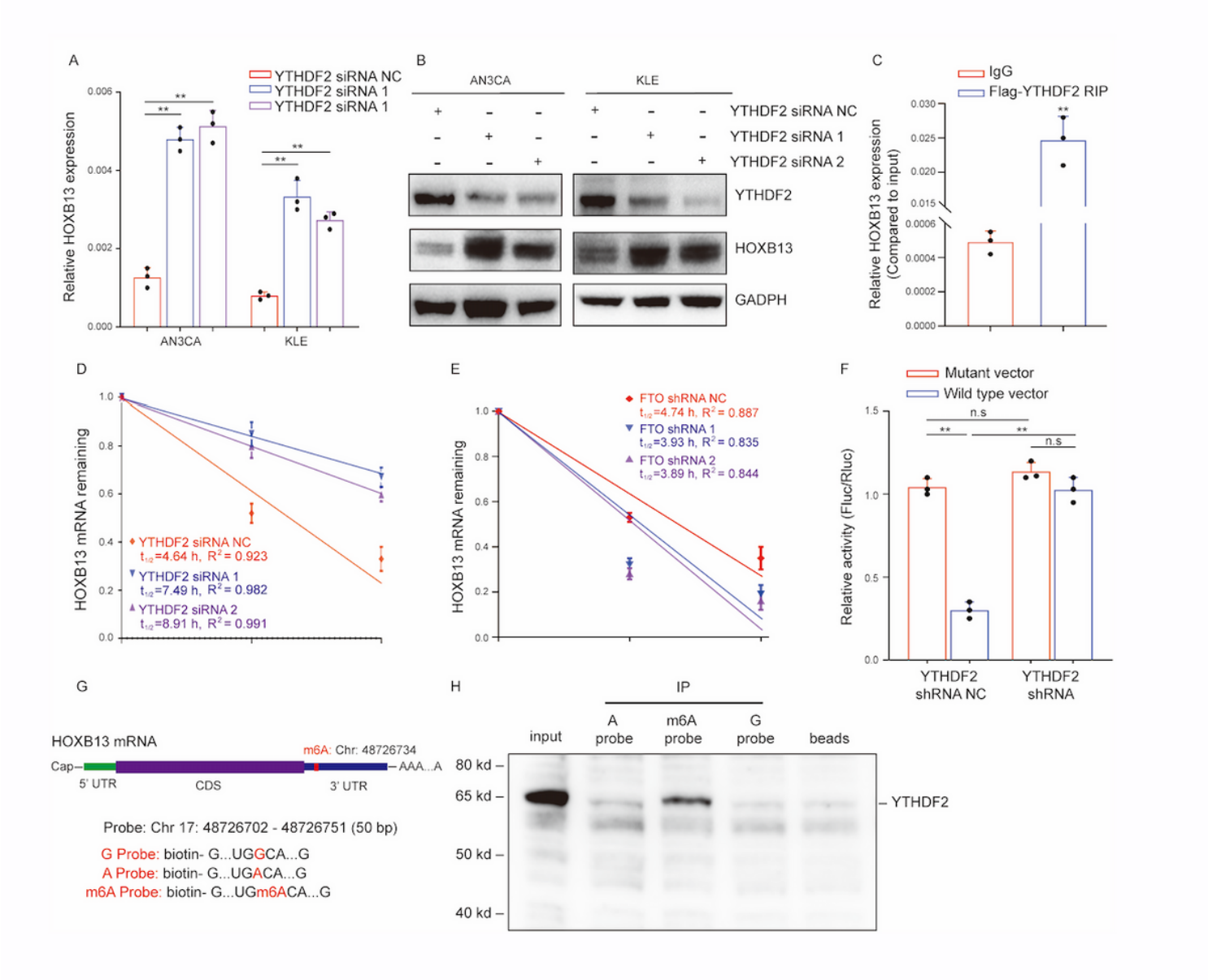

Figure 5

YTHDF2 regulates HOXB13 expression in an m6A-dependent manner. (A, B) qPCR and WB confirmed elevated HOXB13 mRNA and protein expression after YTHDF2 knockdown. (C) RIP-PCR validates exogenous YTHDF2 binding to HOXB13 mRNA. (D) Prolonged RNA lifetime of HOXB13 mRNA after knockdown of YTHDF2 expression. (E) Shortened RNA lifetime of HOXB13 mRNA after knockdown of FTO expression. (F) Relative activity of the wild-type or mutant HOXB13 3' UTR luciferase reporter in AN3CA cells expressing YTHDF2 shRNA or control. (G) Position of the m6A peak in HOXB13 mRNA (top). RNA probe sequences for RNA pulldowns (bottom). (H) YTHDF2 recognizes the m6A site in the 3' UTR of

HOXB13 mRNA as shown by RNA pull-down assays. Error bars indicate means ± SDs, **P<0.01, n.s indicates no significance.

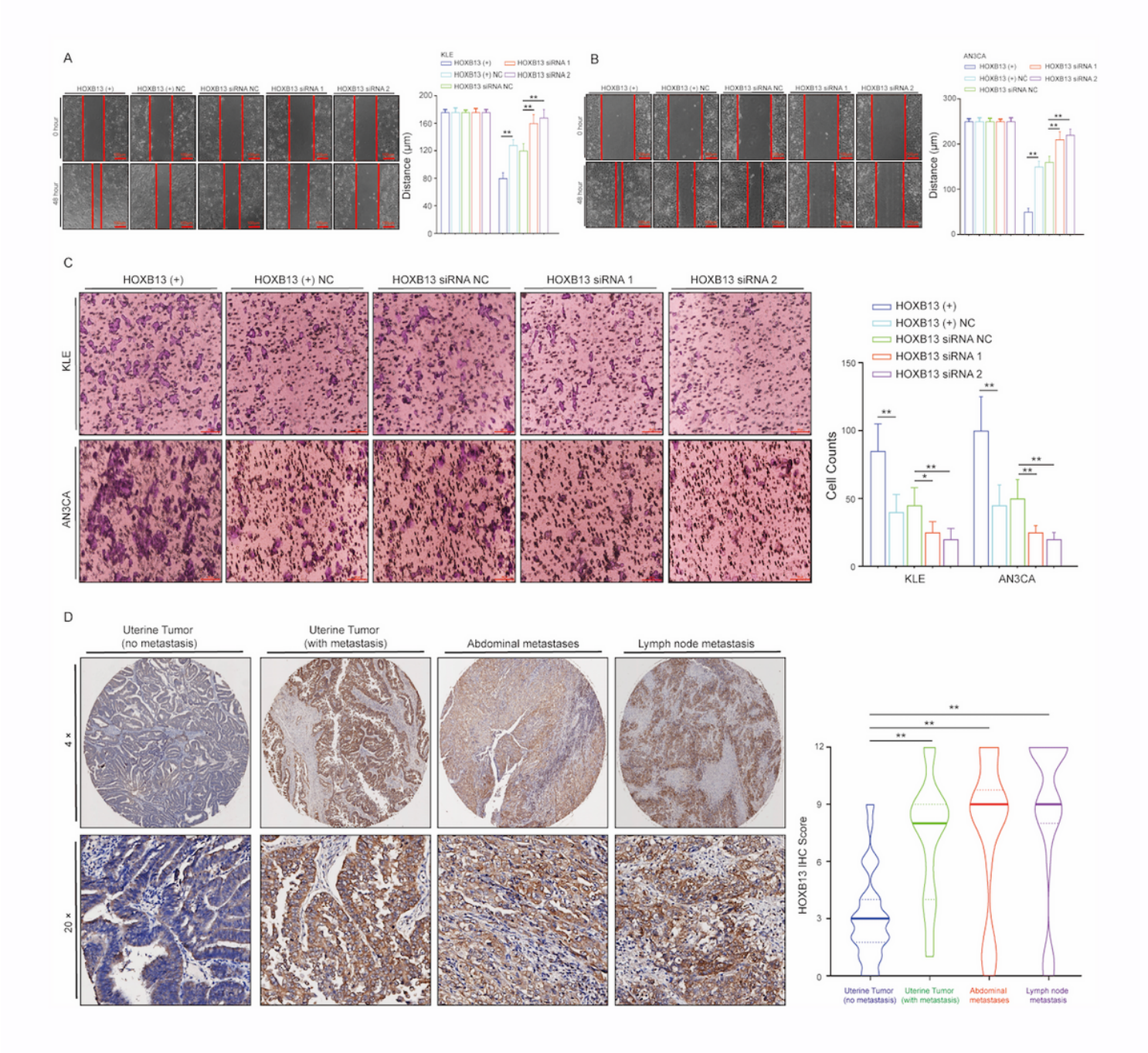

Figure 6

HOXB13 promotes EC cell metastasis and invasion. (A, B) HOXB13 overexpression and knockdown regulate cell migratory abilities in KLE and AN3CA cells by wound-healing assays. (C) Effects of HOXB13 overexpression and knockdown on cell invasive capacities by Transwell assays. (D) Expression of HOXB13 protein in the tissue array validated by IHC. Error bars indicate means ± SDs, **P < 0.01.

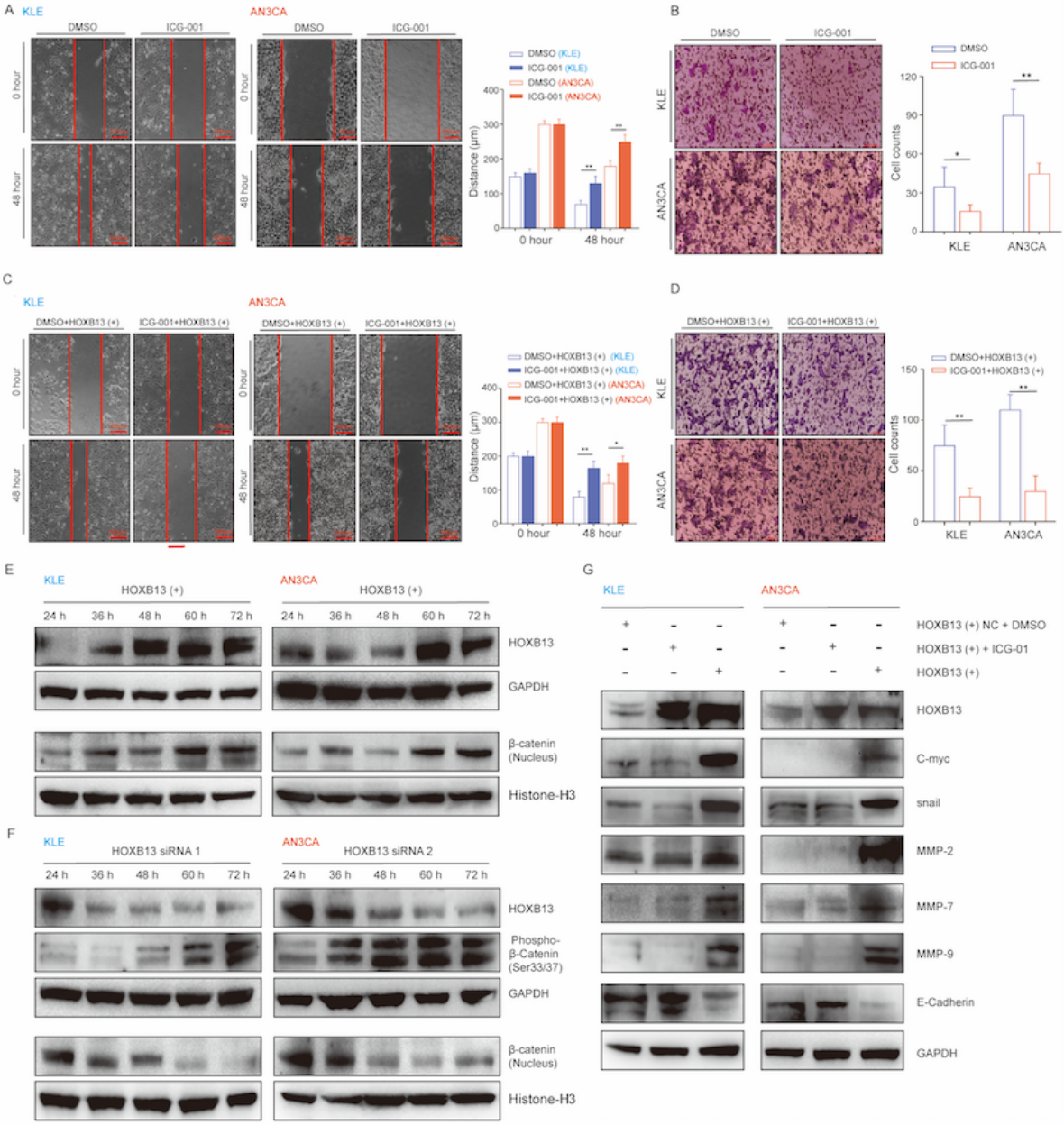

Figure 7

HOXB13 promotes EC cell metastasis and invasion by activating the WNT signaling pathway. (A, B) WNT signaling pathway inhibitor (ICG-001) inhibits metastasis and invasion of KLE and AN3CA cells. (C, D) WNT signaling pathway inhibitor (ICG-001) blocked the effect of promoting tumor cell invasion and metastasis mediated by HOXB13. (E) WB shows that overexpression of HOXB13 promotes β-catenin expression. (F) WB showed phospho-β-catenin (Ser33/37) and β-catenin expression at different time

points after silencing HOXB13 by siRNA. (G) WB showed that a WNT signaling pathway inhibitor (ICG-001) blocked the target genes that were activated by HOXB13 overexpression. Error bars indicate means ± SDs, *P < 0.05, **P < 0.01.

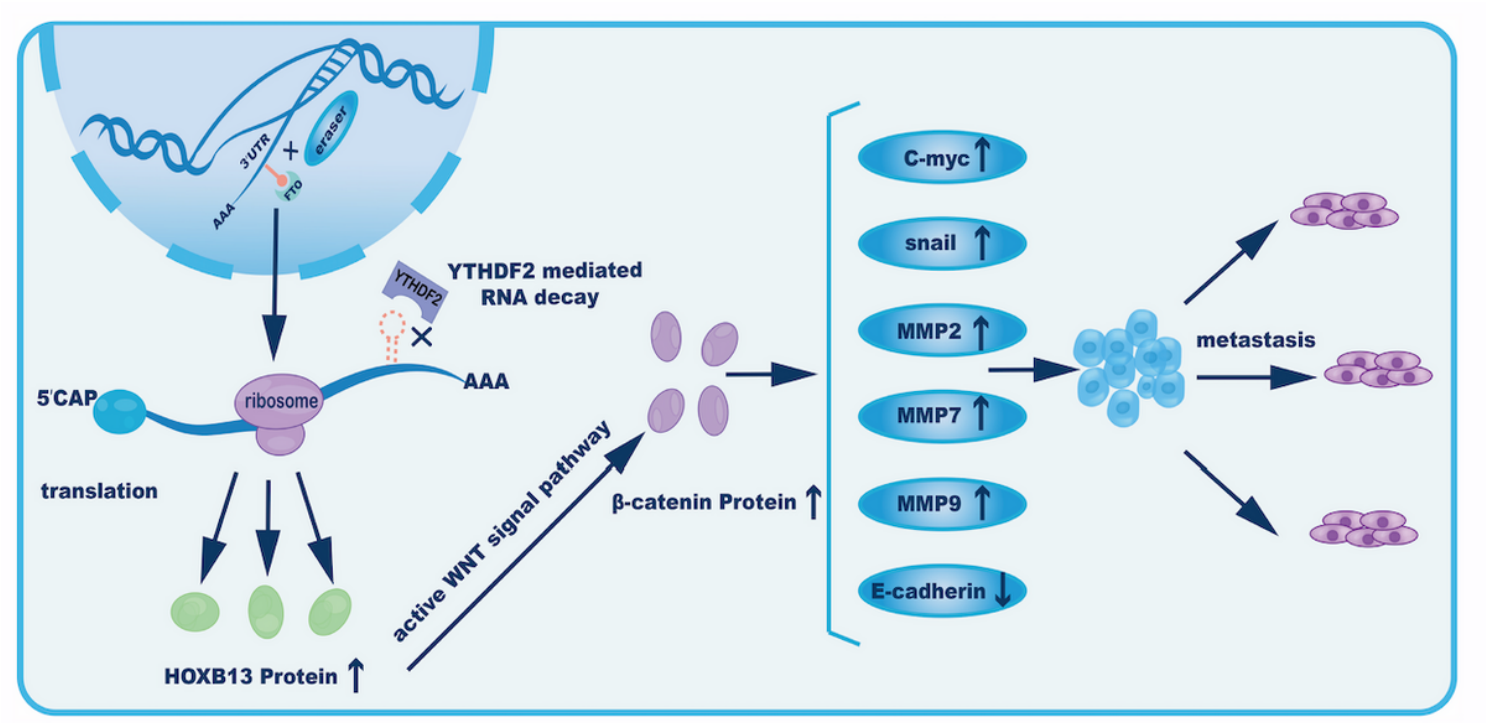

Figure 8

Diagram for the molecular mechanism. This study demonstrate a critical role of FTO in regulating EC metastasis via m6A-HOXB13-WNT mechanism.

Supplementary Files

This is a list of supplementary files associated with this preprint. Click to download.

- Additionalfile5TableS5mRNAseqdata.xlsx
- Additionalfile3TableS3.docx
- Additionalfile7TableS7MeRIPseqdata.xlsx
- Additionalfile8FigureS1.tif
- Additionalfile1TableS1.docx
- Additionalfile2TableS2.docx
- Additionalfile6TableS6RIPseqdata.xlsx
- Additionalfile1TableS1.docx
- Additionalfile2TableS2.docx
- Additionalfile4TableS4.docx

- Additionalfile10FigureS3.tif
- Additionalfile10FigureS3.tif
- Additionalfile9FigureS2.tif
- Additionalfile6TableS6RIPseqdata.xlsx
- Additionalfile4TableS4.docx
- Additionalfile8FigureS1.tif
- Additionalfile7TableS7MeRIPseqdata.xlsx
- Additionalfile5TableS5mRNAseqdata.xlsx
- Additionalfile9FigureS2.tif
- Additionalfile3TableS3.docx